DROPLET SIZE DISTRIBUTIONS OF BIOFUEL SPRAYS

Roger Apaza Vásquez, roger@lcp.inpe.br
Fernanda Francisca Maia, maia@lcp.inpe.br
Fernando de Souza Costa, fernando@lcp.inpe.br
Laboratório de Combustão e Propulsão – LCP
Instituto Nacional de Pesquisas Espaciais – INPE
Rodovia Presidente Dutra km 40, Cachoeira Paulista-SP, Brasil

Abstract. *Environmental concerns motivate the utilization of biofuels in order to reduce the consumption of fossil fuels and to reduce pollutant emissions. Atomizers are devices used to increase the surface area of liquids through the formation of a spray, thus allowing a more efficient vaporization, mixing and burning of liquid fuels. This paper presents and compares droplet size distributions and average diameters, obtained with a dual pressure swirl injector using ethanol and biodiesel through a laser diffraction system.*

Keywords*: Dual pressure swirl injector, ethanol, biodiesel*

1. INTRODUCTION

Because of the uncertain petroleum prices and the impetus to develop renewable energy sources, biofuels are emerging as alternatives to petroleum fuels with practical applicability to gas turbines and industrial combustors. Biofuels have several advantages over conventional fuels such as lower levels of sulfur, presence of oxygen in their molecules, higher cetane number, and less harmful emissions (Aksoy, 2011).

Injectors are used in combustion processes to increase the surface area of the liquids through the formation of a spray, to provide a more efficient vaporization, mixing and burning of liquid fuels. A spray with small droplets of approximately constant diameter allows more uniform burning and uniform heat release distribution in a combustion chamber. Therefore, the droplet size distribution and the average droplet size of a spray are important characteristics in controlling the efficiency of combustion and production of pollutants.

This work describes and compares the droplet size characteristics of sprays of ethanol and soy biodiesel B100 formed through a dual pressure swirl injector for different injection pressures using a laser diffraction system.

The laser diffraction method consists in determining the angle of scattering of light and the intensity of scattering when droplets pass through the laser beam, since these parameters are directly related to droplet size.

International standard has established that the particle size distributions obtained by this technique are calculated by comparing the dispersion patterns collected from a given sample with a suitable optical model. Traditionally two different models of laser diffraction are used: the Fraunhofer's approximation and Mie's theory.

The Fraunhofer approach considers that the particles measured are opaque and have a light scattering for narrow angles, applicable only for large particles (typically greater than 900 μm).

Mie's theory however, provides the intensities of scattering of all particles, whether small or large, transparent or opaque. It can be analyzed the primary scattering from the particle surface, with the intensity provided by the difference in refractive index between the particles dispersion medium and also the secondary scattering caused by the refraction of light within the particle applying the Mie's theory. (ISO 13320-1, 1999).

The Malvern Spraytec system of laser diffraction (Fig.1) provides a rapid method making use of theoretical optical models mentioned above to evaluate the particle sizes of sprays produced by a fuel injection system. This technique can be classified as non-intrusive and requires no external calibration for the measurements related to the distribution of droplet size.

The Spraytec system offers other advantages for the characterization of spray, such as the data can be acquired more quickly since the system has the ability to acquire data with a frequency of 10 kHz, so that the data distribution droplet size can be collected in real time with a resolution of 100 μs. This allows any change in the size of the drops during the measurement of the sample can be detected; allowing the dynamics of atomization is evaluated. Finally, the measurement range of the instrument to the drops is large (0.1 to 2000 μm), ensuring that both the large and small droplets can be detected with a single measurement (Elissev et al, 2008). The algorithm used for analyzing the spreading of drops in the Spraytec system takes into account the multiple scattering which can occur in dense sprays.

1.1 Sauter mean diameter

An average size commonly used in heat and mass transfer processes is the Sauter mean diameter which is proportional to the volume-surface area ratio of all droplets in the spray (Sowa, 1992). The random nature of the atomization process involves several varieties of drop sizes that are produced during the injection of the liquid. The distribution of droplet sizes is of vital importance for the efficiency of the combustion chamber, since, in many cases, for larger drop sizes there is an increase in emissions of NOx.

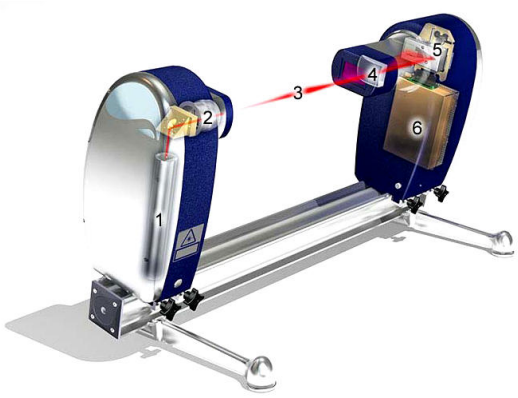

Figure 1. System Spraytec laser diffraction Malvern Company: (1) laser light source, (2) optical collimation, (3) region of measurement, (4) data collectors lenses, (5) light scattering detector, (6) electronics for data acquisition.

This work analyses the droplet size diameter in a dual pressure swirl injector which has two coaxial vortex chambers: primary and a secondary vortex chambers. Each chamber is equivalent to a simple pressure swirl injector, as described by Lefbvre (1989).

Several formulations were developed by different authors to predict the Sauter mean diameter (SMD) in a simple pressure swirl injector, as depicted in Table 1.

Table 1. Formulations used to predict the Sauter mean diameter.

Author	Formulation	Author's Consideration
Couto Carvalho	$\left(\frac{3\pi}{\sqrt{2}}\right)^{0.33} d_{lig}\left[1+\frac{3\mu}{\left(\rho\sigma d_{lig}\right)^{0.5}}\right]^{0.16}$	Diameter of the ligament that leaves the injector
Radcliffe	$7.3\sigma^{0.6}\upsilon^{0.16}m_L^{0.25}\Delta P^{-0.4}$	Experimental data, but without considering geometric effects of injector
Jasuja	$4.4\sigma^{0.6}\upsilon^{0.16}m_L^{0.22}\Delta P^{-0.43}$	Experimental data, but without considering geometric effects of injector
Lefebvre	$2.25\sigma^{0.25}\mu^{0.25}m_L^{0.25}\Delta P^{-0.5}\rho_{gas}^{-0.25}$	Flow at the exist of the injector using the Jasuja data
Kennedy	$10^{-3}\sigma\left(6.11+0.32x10^{5}FN\sqrt{\rho}-6.973x10^{-3}\sqrt{\Delta P}+1.89x10^{-6}\Delta P\right)$	Weber numbers greater than 10 and high values of flow
Wang Lefebvre	$4.52\left(\frac{\sigma\mu^2}{\rho_{gas}\Delta P^2}\right)^{0.25}\left(h_s\cos\alpha\right)^{0.25}+0.39\left(\frac{\sigma\rho}{\rho_{gas}\Delta P}\right)^{0.25}\left(h_s\cos\alpha\right)^{0.75}$	Effects of cone angle and blade thickness of liquid formed at the exit of the injector

2. METODOLOGY

The maximum allowed distance between the particles and the lens defines the working distance for the laser diffraction system. This definition is made by considering the allowed maximum angle scattering (which refers to the detection limit for small particles) and the physical size of the lens (working distance can be higher by increasing the diameter of the lens). In the case of 300 mm lens used in Spraytec, the minimum average particle (Dv_{50}), which can be measured to a spray is 0.5 µm, therefore the maximum working distance is 150 mm in the case where the particles with these dimensions are measured correctly.

The physical-chemical parameters of the biofuels used in the tests are presented in Table 1. They are necessary to obtain the theoretical droplet diameters given by Equation in Table 1. The software supplied by Malvern Company requires the input of density values and refraction indices of the liquids atomized. Once done this, the equipment starts automatically configuring the hardware, the alignment of optics, the sample measurement and processing of results. The measurement can be monitored in real time, so that all aspects of the analysis process are monitored. Once the analysis in complete, a histogram of the "droplet size" collected pertaining to distribution is obtained, allowing a more detailed inspection in time to collect data and monitor the temporal evolution of droplet size measured.

Table 2. Physical-chemical parameters of ethanol and biodiesel.

Biofuel	Density $[kg/m^3]$	Viscosity $[Ns/m^2]$	Surface tension $[N/m]$	**IR**
Ethanol 96 %	806.7	1.24E-03	0.024	1,361
Soy Biodiesel B100	875.7	4.88E-03	0.028	1,476

To validate the data obtained with the laser measuring instrument Malvern injection tests were carried out with distilled water, varying the spatial position of the injector nozzle with respect to the laser beam.

The Malvern Spraytec system allows the transmission and reception modules to be moved into different positions along the base of the tool bar, in order to allow the characterization of a wide variety of sprays. Therefore the horizontal positioning of the injector nozzle with respect to the receiver module should be considered. It is important to determine the effect of the horizontal displacement is performed when the measurement of droplet size since the position may affect the accuracy of measurements made with the laser diffraction instrument.

In particular, if the distance between the spray and the optical receiver module of the instrument is too large it may not be possible to accurately measure smaller particles within the measurement zone. To determine the effect of spatial position of the injector on the measurement of spray generated by this, some measurements were made for certain horizontal distances from the receiver module of the instrument maintaining constant vertical distance of 78 mm between the exit nozzle of the injector and the laser beam emitted by the transmitter module of the instrument using distilled water as liquid injection at a pressure of 1.6 bar for all measurements performed.

3. RESULTS AND DISCUSSION

The vertical and horizontal positions of the injector were varied to establish a measurement range with almost constant droplet diameters where the laser diffraction measurements were accurate and reliable. Therefore, the spatial position of the injector nozzle chosen for all measurements was 180 mm from the receiver module of the laser diffraction instrument and 95 mm above the horizontal line of the laser beam emitted by the transmission module of the instrument. Fig. 2 shows the spatial location of the injector with the laser beam emitted by the laser diffraction instrument.

Figure 2. View of the injector with the laser beam emitted from the Spraytec laser system.

3.1 Results for the mean diameters of droplets with ethanol injection

Measurements were taken of the Sauter diameter as a function of injection pressure only in the primary chamber for hydrated ethanol, because ethanol droplets generated by the injector in the secondary chamber would wet the cover glass receiver of the instrument of laser diffraction. Despite searching for an optimum position of the exit of injector with respect to the laser beam the corresponding measurements could not be performed due to limitations of the horizontal length of the bar base Spraytec.

Figure 3 compares experimental and theoretical results of the SMD in the injector primary chamber with injection of ethanol at different pressures. It is seen that the Couto-Carvalho equation could not correctly predict the behavior of Sauter diameter of hydrated ethanol.

The cumulative distributions of volume and the characteristic diameters of droplets formed by the injection of ethanol at the primary chamber can be seen in Fig. 4 and the probability density functions (frequency) of the diameters of the drops in Fig. 5 both for different injection pressures (manometric).

It can be observed in these Figures that the characteristic average diameter of droplets of hydrous ethanol, such as SMD, Dv_{10}, Dv_{50} and Dv_{90}, decrease with increasing injection pressure and that the cumulative volume distributions and functions of probability distribution (frequency) of the diameters of the drops moving to the left with increasing pressure, also indicating a reduction in the average diameters of the drops.

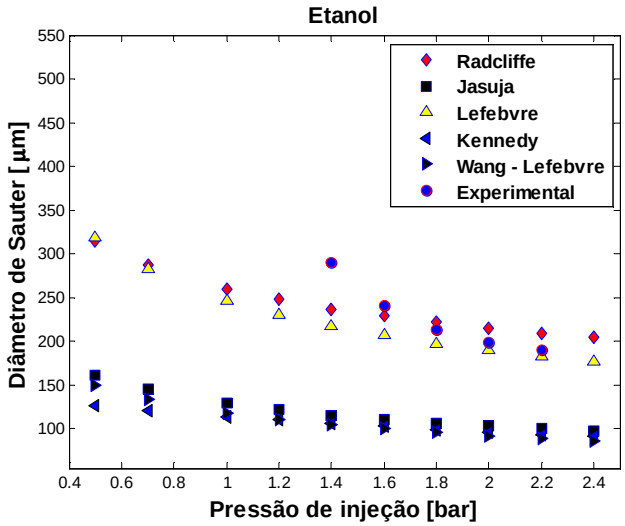

Figure 3. Comparisons of theoretical results and experimental SMD data for the injection of hydrated ethanol in the primary chamber.

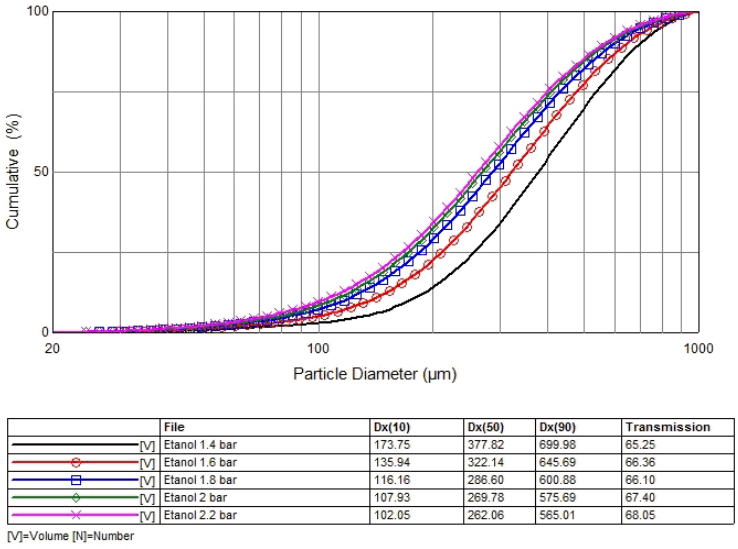

	File	Dx(10)	Dx(50)	Dx(90)	Transmission
[V]	Etanol 1.4 bar	173.75	377.82	699.98	65.25
[V]	Etanol 1.6 bar	135.94	322.14	645.69	66.36
[V]	Etanol 1.8 bar	116.16	286.60	600.88	66.10
[V]	Etanol 2 bar	107.93	269.78	575.69	67.40
[V]	Etanol 2.2 bar	102.05	262.06	565.01	68.05

Figure 4. Cumulative distributions of ethanol droplet diameters with different pressures in the injector primary chamber.

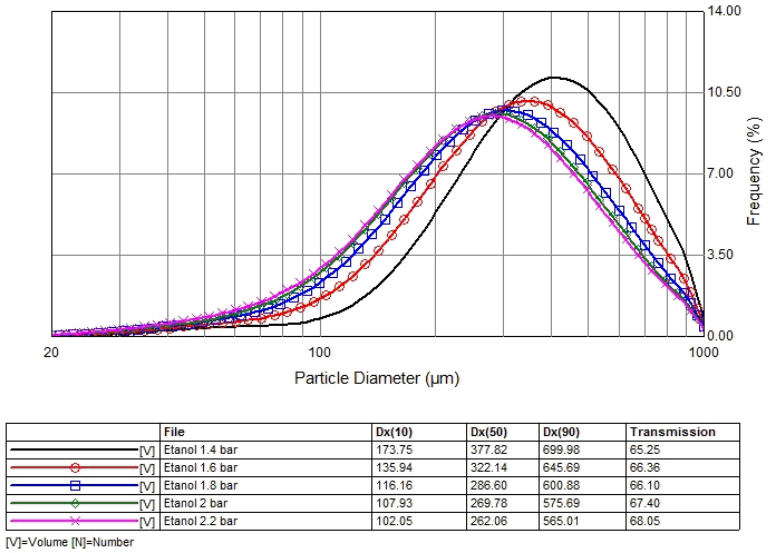

	File	Dx(10)	Dx(50)	Dx(90)	Transmission
[V]	Etanol 1.4 bar	173.75	377.82	699.98	65.25
[V]	Etanol 1.6 bar	135.94	322.14	645.69	66.36
[V]	Etanol 1.8 bar	116.16	286.60	600.88	66.10
[V]	Etanol 2 bar	107.93	269.78	575.69	67.40
[V]	Etanol 2.2 bar	102.05	262.06	565.01	68.05

[V]=Volume [N]=Number

Figure 5. Frequency curves of ethanol droplet diameters with different pressures in the injector primary chamber.

3.2 Results for the mean diameters of droplets with biodiesel injection

Figure 6 compares the experimental values of the SMD of the drops of soy biodiesel B100 injected into the primary chamber with the theoretical values of the different semi-empirical equations for different injection pressures (manometric).

None of the semi-empirical equations are able to correctly predict the SMD for biodiesel B100. The Radcliffe equation seems to indicate a trend toward a behavior similar to experimental SMD for higher pressures. Since the equations mentioned were developed using mostly water as liquid injection, or in some cases liquids with low viscosity, one can assume that they must not generate the same experimental behavior for high viscosity liquids.

The cumulative distributions of volume and the characteristic diameters of droplets formed by the injection of ethanol at the primary chamber and the probability density functions (frequency) of the diameters for different injection pressures (manometric) can be seen in Figs. 7 and 8, respectively.

The characteristic mean diameter decreases with increasing the injection pressure and the cumulative distributions of volume and the distribution functions of probability (frequency) of the diameters of the drops of biodiesel is moving to the left with increasing pressure, indicating a reduction in the average diameters of the drops, just as occurred with the injection of hydrated ethanol.

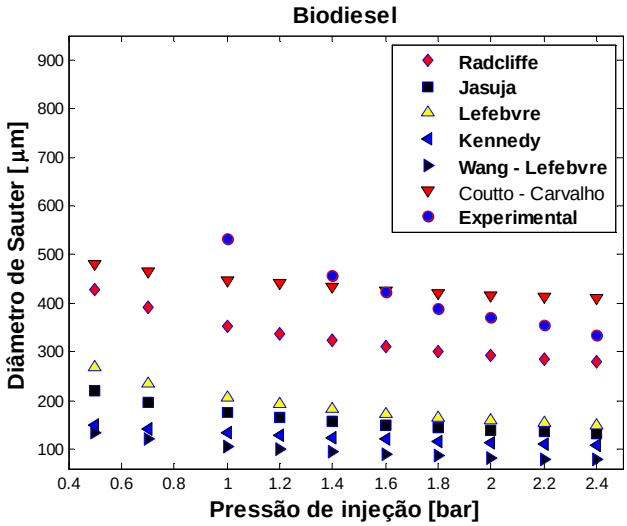

Figure 6. Comparisons of theoretical formulations and experimental SMD data for injection of soy biodiesel B100 in the primary chamber.

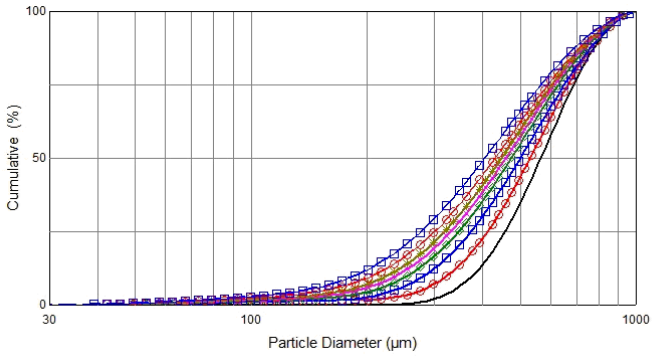

	File	Dx(10)	Dx(50)	Dx(90)	Transmission
[V]	Biodiesel 1 bar	375.39	564.94	798.73	86.49
[V]	Biodiesel 1.4 bar	322.63	529.96	788.29	81.11
[V]	Biodiesel 1.6 bar	280.82	499.83	787.84	83.87
[V]	Biodiesel 1.8 bar	254.55	473.38	768.98	85.27
[V]	Biodiesel 2 bar	237.68	457.95	758.38	85.57
[V]	Biodiesel 2.2 bar	225.45	446.00	750.44	85.81
[V]	Biodiesel 2.4 bar	207.04	429.85	743.59	85.89
[V]	Biodiesel 2.6 bar	186.39	404.76	724.31	85.78

[V]=Volume [N]=Number

Figure 7. Cumulative distribution of soy biodiesel droplet diameters with different pressures in the primary chamber.

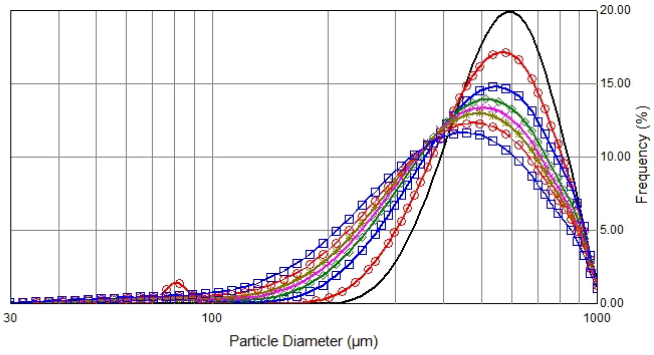

	File	Dx(10)	Dx(50)	Dx(90)	Transmission
[V]	Biodiesel 1 bar	375.39	564.94	798.73	86.49
[V]	Biodiesel 1.4 bar	322.63	529.96	788.29	81.11
[V]	Biodiesel 1.6 bar	280.82	499.83	787.84	83.87
[V]	Biodiesel 1.8 bar	254.55	473.38	768.98	85.27
[V]	Biodiesel 2 bar	237.68	457.95	758.38	85.57
[V]	Biodiesel 2.2 bar	225.45	446.00	750.44	85.81
[V]	Biodiesel 2.4 bar	207.04	429.85	743.59	85.89
[V]	Biodiesel 2.6 bar	186.39	404.76	724.31	85.78

[V]=Volume [N]=Number

Figure 8. Frequency curves of soy biodiesel droplet diameters with different pressures in the primary chamber.

3.3 Results for ethanol injection in the primary chamber and biodiesel in the secondary chamber

Figure 9 shows SMD results for the injection of ethanol in the primary chamber and biodiesel in the secondary chamber, with the same injection pressure in both chambers.

It can be seen in Fig. 9 that the behavior of Sauter diameter of the mixture is quite different from the results obtained for each chamber individually (see Fig. 3 for the case of ethanol). In this case we can see that when there is a pressure increase the size of the Sauter diameter tends to diminish what is a common behavior in simple pressure swirl injectors.

When the two chambers work together, the behavior shown in Fig. 9 indicates that when the two spray cones are attached or experiences a separation, the distribution of droplet size is influenced as described Sivakumar and Raghunandan (1998). They observed that for a given fixed mass flow from the primary chamber and increasing the mass flow of the secondary chamber, the average size of the drop initially increases until it reaches a maximum and then begins to decrease.

It was observed in this study that the liquid film generated in the primary chamber with hydrated ethanol influences the droplet size only for low values of mass flow rates of the secondary camera using soy biodiesel. If soy biodiesel was used in the primary chamber and ethanol in the secondary chamber, the two liquid cones could not collide properly and mix the two fuels.

Figure 10 shows cumulative distributions of volume for the injection of mixtures of hydrated ethanol and biodiesel in the dual centrifugal injector at different injection pressures. Figure 11 shows the frequency curves of diameters.

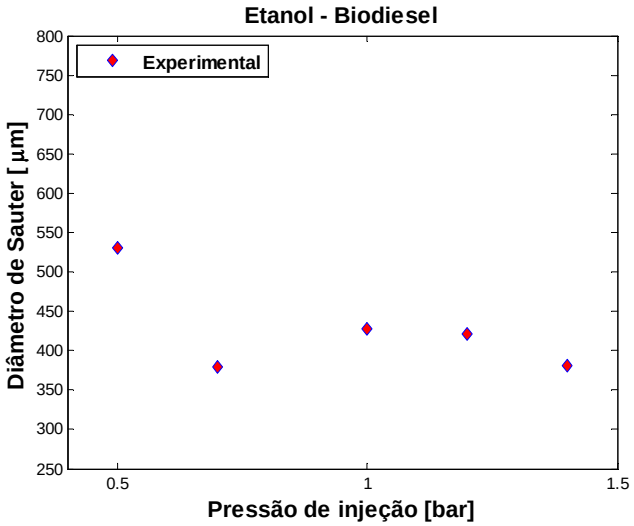

Figure 9. SMD of the mixture of hydrated ethanol and B100 soy biodiesel at different pressures applied to the dual pressure swirl injector.

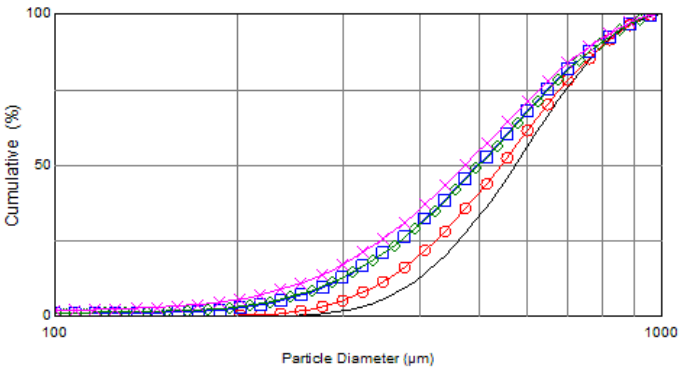

	File	Dx(10)	Dx(50)	Dx(90)	Transmission
[V]	Biodiesel - etanol 05bar	380.54	573.25	802.64	87.88
[V]	Biodiesel - etanol 07bar	336.95	543.10	804.57	88.36
[V]	Biodiesel - etanol 1bar	278.66	497.56	786.66	86.88
[V]	Biodiesel - etanol 1,2bar	276.56	500.25	789.14	79.29
[V]	Biodiesel - etanol 1,4bar	245.60	474.64	771.81	78.70

[V]=Volume [N]=Number

Figure 10. Cumulative distributions of the mixture of hydrated ethanol and soy biodiesel droplets with different injection pressures.

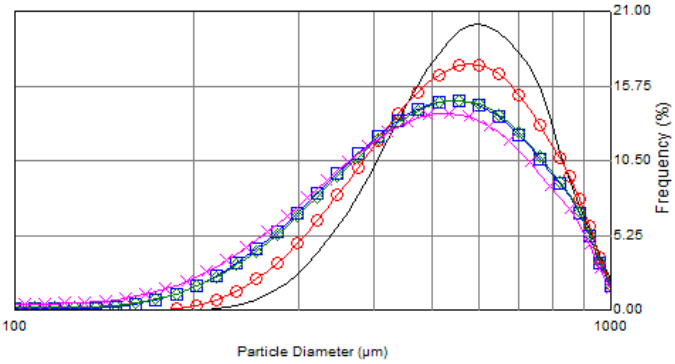

	File	Dx(10)	Dx(50)	Dx(90)	Transmission
[V]	Biodiesel - etanol 05bar	380.54	573.25	802.64	87.88
[V]	Biodiesel - etanol 07bar	336.95	543.10	804.57	88.36
[V]	Biodiesel - etanol 1bar	278.66	497.56	786.66	86.88
[V]	Biodiesel - etanol 1.2bar	276.56	500.25	789.14	79.29
[V]	Biodiesel - etanol 1.4bar	245.60	474.64	771.81	78.70

[V]=Volume [N]=Number

Figure 11. Frequency curves of droplet diameters for the mixture of hydrated ethanol and soy biodiesel with different injection pressures.

4. CONCLUSIONS

This paper presented and compared characteristics of sprays of biofuels injected through a dual pressure swirl injector. Experimental data and theoretical values of the Sauter Mean Diameters of droplets of hydrated ethanol and B100 soy biodiesel were compared for different injection pressures. Volume average droplet diameters, cumulative distributions and curves of diameter frequencies were presented.

5. ACKNOWLEDGMENTS

The authors acknowledge CAPES through the Pró-Engenharia Program for providing a scholarship to the first author.

6. REFERENCES

Aksoy, F., 2011. “The effect of opium poppy oil diesel fuel mixture on engine performance and emissions”, Int. J. Environ. Sci. Tech, Vol. 8, No. 1, pp. 57-62.

Bazarov, V., Vigor, Y., Puri, P., 2004. “Design and Dynamics of Jet and Swirl Injectors, Liquid Rocket Thrust Chambers: Aspects of Modeling, Analysis, and Design”. USA : American Institute of Aeronautics and Astronautics.

Chen, S. K., Lefebvre, A. H., Rollbuhler, J., 1991. “Influence of liquid viscosity on pressure-swirl atomizer performance”, Atomization and Sprays, Vol. 1, pp. 1 – 22.

Couto, H. S., Carvalho Jr, J. A., Bastos – Netto, D., 1997. “Theoretical formulation for Sauter mean diameter of pressure-swirl atomizers”, Journal Propulsion and Power, Vol. 13, No. 5, pp. 691 – 196.

Eliseeva, O. A., Sister, V. G., Orlov, S. V., 2008. “Measurement of the fractional composition of two-phase systems with determination of the efficiency of separation processes”, Chemical and Petroleum Engineering, Vol. 44, pp. 722-725.

Lefebvre, A. H., 1989. “Atomization and Sprays”, Hemisphere, New York, USA.

Sowa, W. A., 1992. “Interpreting mean drop diameters using distribution moments”, Atomization and Sprays, Vol. 2, pp. 1 – 15.

Wang, X. F., Lefebvre, A. H., 1987. “Mean drop sizes from pressure-swirl nozzles”, Journal of Propulsion Power, Vol. 3, No. 1, pp. 11-18.

6. RESPONSIBILITY NOTICE

The authors are the only responsible for the printed material included in this paper.